

University of Bath
Department of Mechanical Engineering

Aerofoil Laboratory Report

Elliot Routier

er909

ME20022

November 1, 2024

Lab Group 10

Word Count: 1923

Summary

This experiment examined the relationship between pressure distribution and angle of attack for a NACA 2415 aerofoil, with the aim of comparing it to NACA data and experimentally understand the effects of implementing a leading-edge slat. It was determined that the lift coefficient increases linearly with the angle of attack for any given Reynolds. However, as the Reynolds number increases, the maximum achievable lift coefficient also increases resulting in a delayed stall angle. Additionally, deploying a slat on the leading-edge of the aerofoil dramatically increases the maximum lift coefficient and further delays the stall angle.

Contents

Summary.....	1
Introduction.....	3
Experimental Apparatus and Procedure.....	5
Results.....	7
Discussion.....	12
Conclusion.....	14
References.....	15
Appendix.....	16

Figures

Figure 1.....	4
Figure 2.....	5
Figure 3.....	5
Figure 4.....	6
Figure 5.....	6
Figure 6.....	8
Figure 7.....	9
Figure 8.....	11
Figure 9.....	13
Figure 10.....	13
Figure 11.....	14

Equations

Equation 1.....	3
Equation 2.....	3
Equation 3.....	3
Equation 4.....	3
Equation 5.....	4

Tables

Table 1.....	7
Table 2.....	10

Introduction

On 17 December 1903 bicycle mechanics, the Wright brothers, piloted the first aeroplane along a 60-foot launch rail. The Wright Flyer was a wood and canvas aeroplane powered by a 12 horse-power petrol engine, connected to two large propellers with, bicycle chains. The machine lifted into the air, rising suddenly to 10 feet, then flew erratically for 12 seconds, landing 120 feet from the starting point. This milestone marked the beginning of humankind's quest to advance flight performance, a journey that led, 66 years later, to Neil Armstrong's first step on the moon [1].

Much of the progress involved in flight performance has centred around aerofoils, a specially designed structure that interacts with airflow to create lift, making them a fundamental aspect of wings and an important concept in aerodynamics, as described by Arthur Baret [2].

An aerofoil is an asymmetric component with a curved upper surface and a flatter lower surface composed of a leading edge and a trailing edge. Lift on an aerofoil is generated by pressure difference between its upper and lower surfaces. The theory is explained from Bernoulli's principle, which states that faster airflow results in lower local pressure.

Equation 1, Bernoulli's equation for an incompressible, inviscid flow

$$P_{\infty} + \frac{\rho U_{\infty}^2}{2} = P + \frac{\rho U^2}{2}$$

The local static pressure at any point on the aerofoil can be represented non-dimensionally in terms of the coefficient of pressure, C_p :

Equation 2, the coefficient of pressure represented non-dimensionally

$$C_p = \frac{P - P_{\infty}}{\frac{1}{2} \rho U_{\infty}^2}$$

The angle of attack of an aerofoil, defined as the angle between the oncoming airflow and the aerofoil's chord line, also affects lift. However, at higher angles of attack, boundary layer separation can occur causing a loss of lift and potentially resulting in stall.

The lift force is quantified by a non-dimensional coefficient of lift, C_L :

Equation 3, the lift coefficient represented non-dimensionally

$$C_L = \frac{L}{\frac{1}{2} \rho U_{\infty}^2 S}$$

Where the wing area for a two-dimensional aerofoil is represented by

Equation 4, wing area for a two-dimensional aerofoil

$$S = c \times 1.0$$

where c is the aerofoil chord.

Lift coefficients can be plotted against various angles of attack to gain an understanding in the lift generated by an aerofoil depending on its inclination.

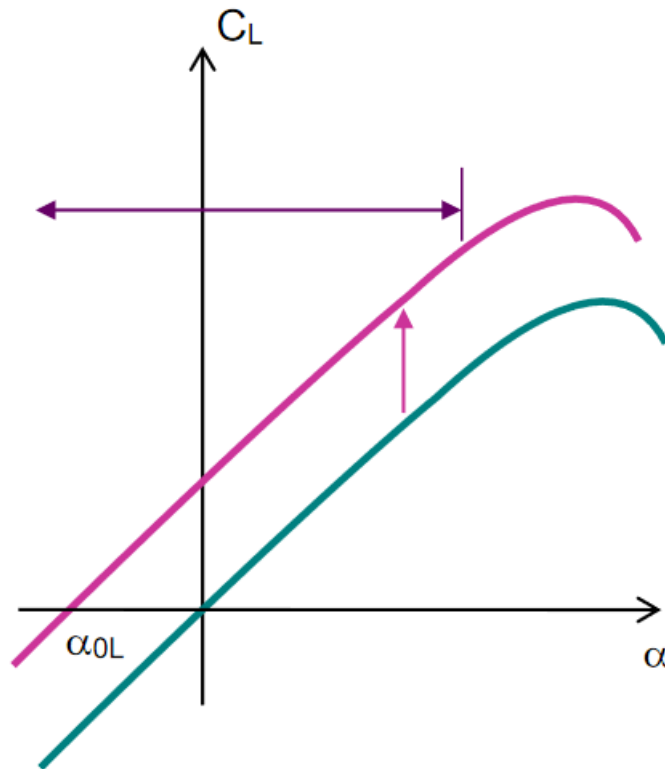


Figure 1 (from handout [3]): A plot of lift coefficient against a range of angles of attack

The Reynolds number provides insight into the relationship between inertial and viscous forces in the fluid. It helps determine how these forces interact, influencing pressure distribution along the aerofoil surface.

Equation 5, the Reynolds number is a non-dimensional quantity that represents the relationship between inertial and viscous forces.

$$Re = \frac{\rho u L}{\mu}$$

Higher Reynolds numbers indicate a greater influence of inertial forces, which can improve boundary layer attachment to the aerofoil surface, thus enhancing lift.

Experimental Apparatus and Procedure

In this experiment, the NACA 2415 aerofoil was tested in a wind tunnel. The NACA 2415 aerofoil has a 2% camber and a 10% thickness where the maximum camber is located at 40% of the chord and the maximum thickness at 15% of the chord.

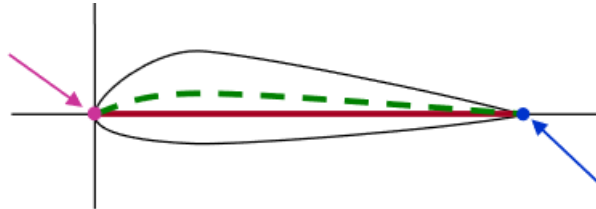


Figure 2: Visualisation of the NACA 2415 aerofoil showing its chord length, camber location, leading-edge and trailing edge.

The wind tunnel, operating at a flow speed of approximately 20 m/s, uses a honeycomb structure to straighten and stabilise the flow entering the test section. The NACA 2415 aerofoil was placed in the test section of the wind tunnel and equipped with 33 pressure taps along its surface.



Figure 3: Image showing the 33 pressure taps on the aerofoil that are connected to a pressure transducer. The transducer outputs signals to the Scanivalve program, enabling measurements of the pressure distribution over the aerofoil.

These pressure taps were connected to a pressure transducer that converts pressure measurements into electrical signals. The pressure transducer was calibrated before the start of the experiment.



Figure 4: The pressure transducer connected to the 33 pressure taps on the aerofoil.

The transducer was linked to a computer system that collected this data. The data was then processed by the Scanivalve program that performed trapezoidal integration to measure values of C_l and C_p for different angles of attack ranging from -10° to 20° in steps of 1° using a manual dial. Further values of C_l and C_p were recorded for the aerofoil fitted with a leading-edge slat at a 15° angle of attack.



Figure 5: The Scanivalve programme receiving data from the pressure transducer. This program performed trapezoidal integration to interpolate the pressure distribution over the aerofoil from the 33 pressure taps.

Results

Lift Coefficient - Lab Data and NACA Data					
Angle (°)	Reynolds Number				
	172,861		3,000,000	6,000,000	9,000,000
	w/o slat	with slat	w/o slat	w/o slat	w/o slat
-18				-0.9	
-17				-1.15	
-16				-1.35	
-15					
-14				-1.25	
-13					
-12				-1.05	
-11					
-10	-0.79		-0.825	-0.825	-0.875
-9	-0.801				
-8	-0.736		-0.625	-0.625	-0.675
-7	-0.708				
-6	-0.495		-0.4	-0.4	-0.45
-5	-0.298				
-4	-0.209		-0.225	-0.225	-0.225
-3	-0.065				
-2	0.009		0	0	0
-1	0.124				
0	0.209		0.2	0.2	0.225
1	0.354				
2	0.44		0.4	0.4	0.425
3	0.602				
4	0.697		0.625	0.625	0.625
5	0.805				
6	0.876		0.8	0.8	0.85
7	1.001				
8	1.026		1	1.025	1.075
9	1.122				
10	1.178	1.28	1.2	1.2	1.275
11	1.22	1.424			
12	1.239	1.394	1.3	1.4	1.425
13	1.217	1.566			
14	1.189	1.641	1.425	1.5	1.57
15	0.989	1.54			
16	1.118	1.57	1.3	1.6	1.65
17	0.921	1.546			
18	0.75	1.277	1.175	1.3	1.575
19	0.786	1.191			
20	0.77	1.209	1.075	1.125	1.35
21					
22			1.025	1.075	1.25
23					
24			1.05	1	1.325

Table 1: Comparison of lift coefficients against angles of attack ranging from -10° to 20° in 1° increments for the experimental data and published NACA data. The NACA data includes angles of attack from -10° to 24° for the Reynolds numbers of 3×10^6 and 9×10^6 , as well as from -18° to 24° for a Reynolds number of 6×10^6 .

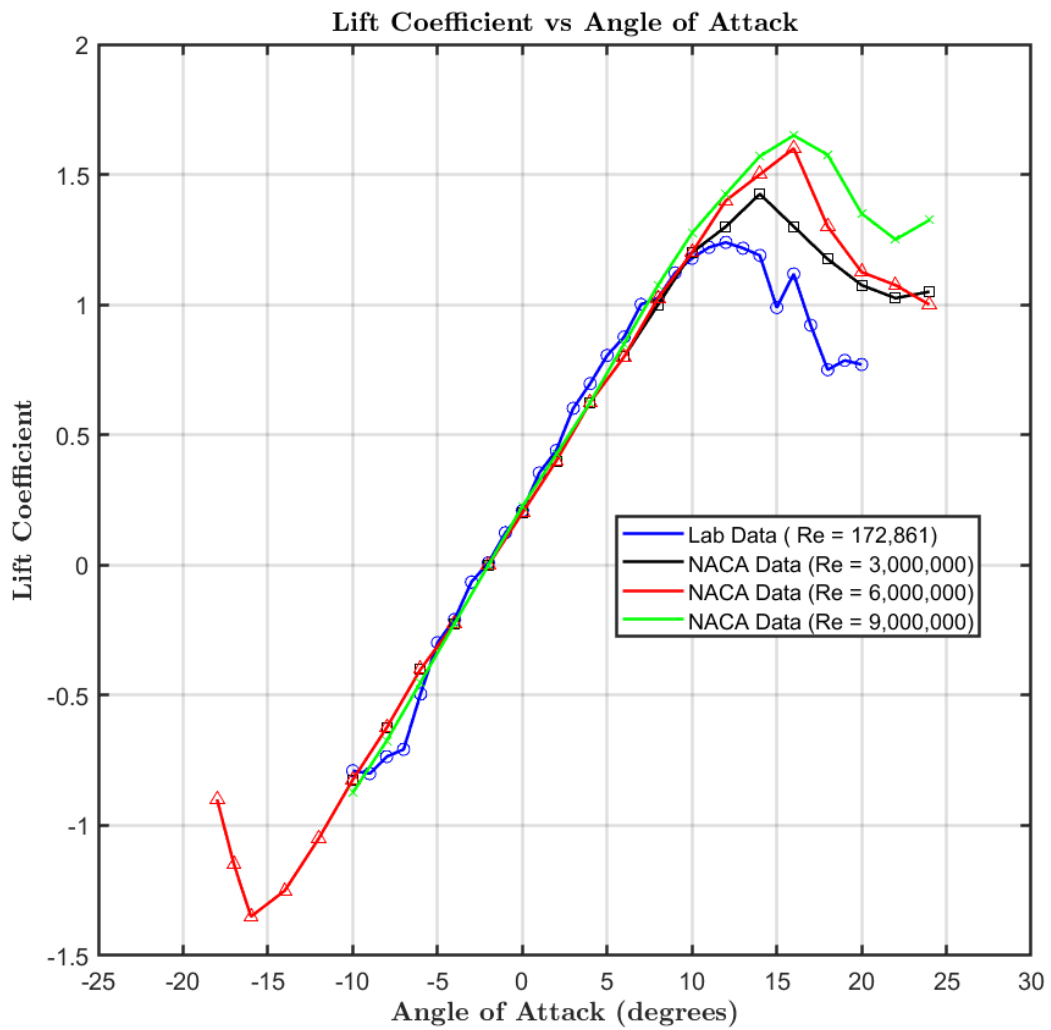


Figure 6: Plot of lift coefficients against angles of attack comparing the experimental data collected during the lab with the NACA data. The gradient of the linear section from the experimental data was 6.26. Comparing this gradient with the theoretical gradient of 2π per radians, the percentage error was found to be 0.40%.

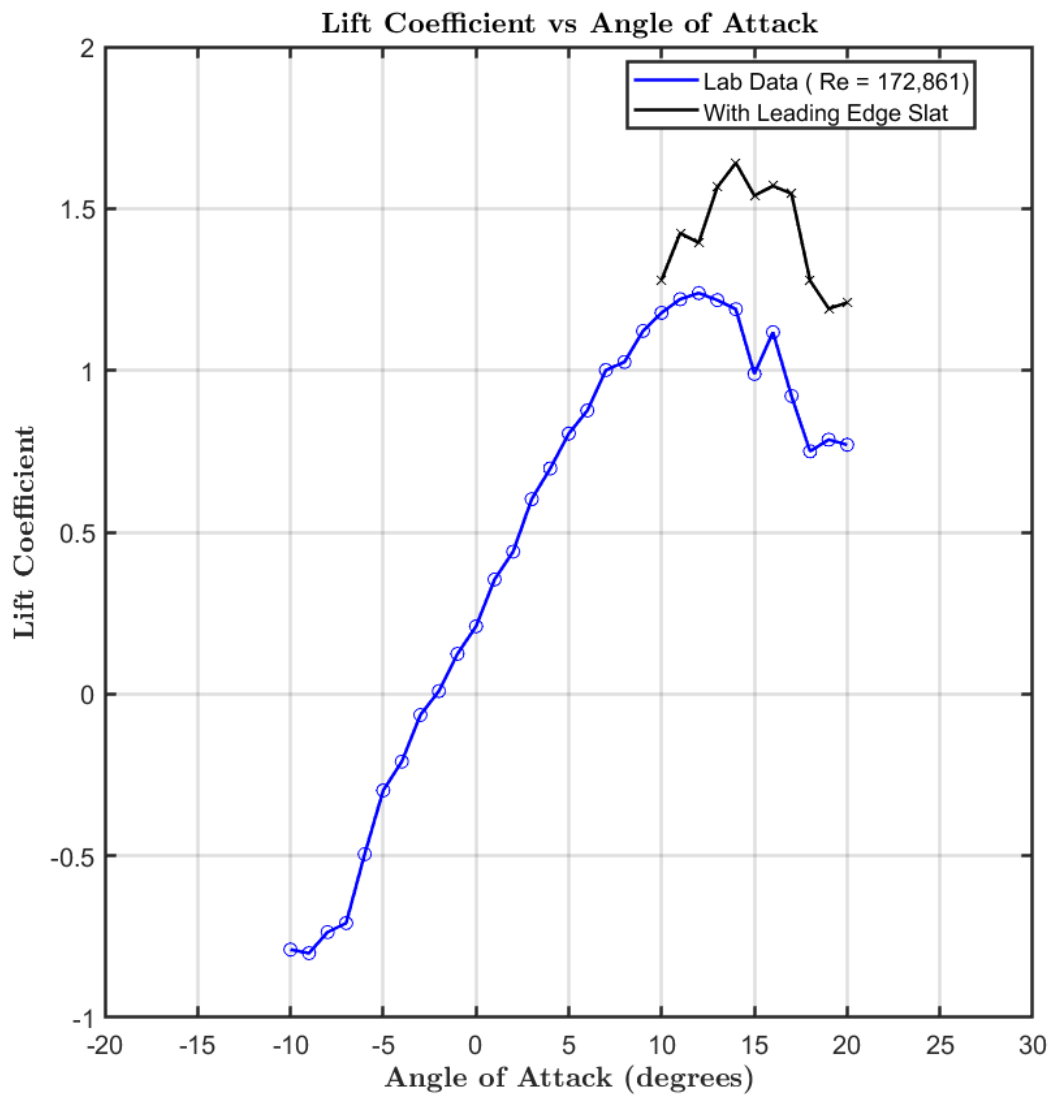
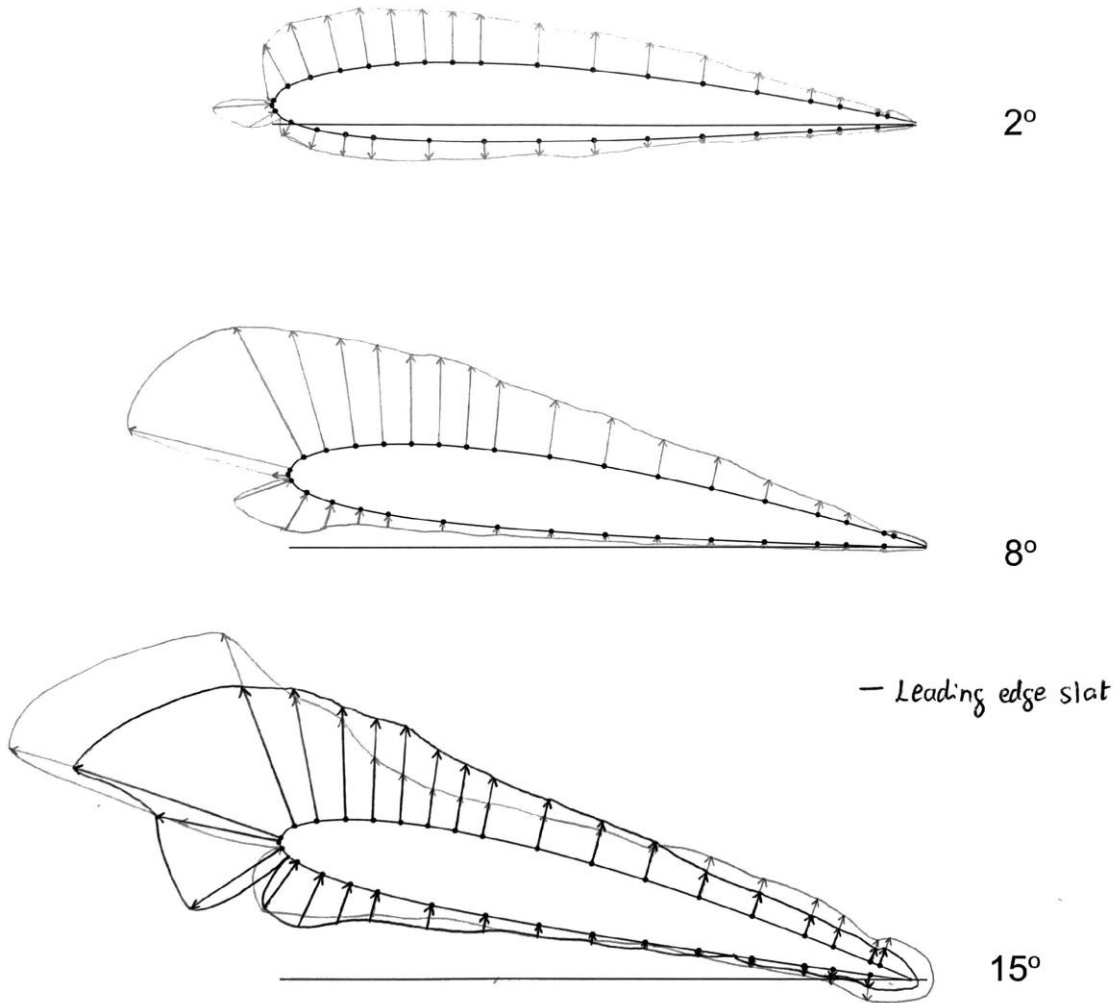


Figure 7: Comparison of lift coefficient versus angle of attack with and without a leading-edge slat. The leading-edge slat data was recorded for angles of attack ranging from 10° to 20° in increments of 1°.

Aerofoil Lab Pressure Coefficient Data - Conventional Aerofoil									
0 degrees		2 degrees		8 degrees		15 degrees		15 degrees (with slat)	
PS	SS	PS	SS	PS	SS	PS	SS	-1.980	-3.351
0.010	0.000	0.548	0.989	0.963	-0.253	0.425	-1.760	0.957	-3.861
0.042	0.010	-0.223	-0.051	0.727	-2.862	0.969	-4.787	0.975	-2.687
0.083	0.043	-0.331	-0.839	0.438	-2.540	0.738	-3.653	0.761	-2.407
0.125	0.080	-0.366	-1.001	0.266	-2.165	0.540	-2.215	0.561	-2.021
0.167	0.125	-0.375	-0.985	0.193	-1.931	0.421	-1.796	0.405	-1.812
0.250	0.167	-0.297	-0.998	0.124	-1.775	0.280	-1.118	0.285	-1.709
0.333	0.208	-0.247	-0.963	0.084	-1.644	0.200	-0.825	0.196	-1.471
0.417	0.250	-0.209	-0.931	0.069	-1.555	0.123	-0.649	0.115	-1.321
0.500	0.291	-0.168	-0.889	0.046	-1.424	0.074	-0.588	0.073	-1.154
0.583	0.333	-0.137	-0.833	0.047	-1.214	0.019	-0.576	0.052	-0.882
0.667	0.417	-0.092	-0.755	0.067	-1.034	-0.023	-0.585	-0.025	-0.753
0.750	0.500	-0.074	-0.656	0.054	-0.871	-0.111	-0.611	-0.085	-0.569
0.833	0.583	-0.054	-0.594	0.045	-0.681	-0.166	-0.578	-0.112	-0.485
0.878	0.667	-0.030	-0.500	0.052	-0.531	-0.245	-0.652	-0.183	-0.435
0.936	0.750	-0.008	-0.309	0.029	-0.375	-0.400	-0.678		-0.374
	0.833		-0.208		-0.203		-0.688		-0.324
	0.878		-0.146		-0.117		-0.639		-0.269
	0.936		-0.018		0.001		-0.408		-0.308
	0.950		0.038		0.034		-0.545		

Table 2: Pressure coefficients recorded for angles of attack at 0, 2, 8 and 15° which are used to sketch the pressure distribution over the NACA 2415 in figure 8.

Aerofoil sketches for pressure-arrow diagrams $1\text{ cm} = 1\text{ }C_p$



Pressure Surface	x/c	0.010	0.042	0.083	0.125	0.167	0.250	0.333	0.417	0.500	0.563	0.667	0.750	0.833	0.878	0.936				
Suction Surface	x/c	0.000	0.010	0.043	0.080	0.128	0.167	0.208	0.260	0.291	0.333	0.417	0.500	0.583	0.667	0.750	0.833	0.878	0.936	0.950

Figure 8: Visualisation of the pressure distribution over the aerofoil for angles of attack ranging from 2, 8 and 15°. The third sketch illustrates two pressure distributions at 15°: one without a leading-edge slat and one with a leading-edge slat.

Experimental uncertainty is an inherent consideration in any laboratory setting. In this experiment, several sources of uncertainty were identified:

1. **Angle of Attack Adjustment:** The angle of attack was increased from -10 to 20° in 1° increments using a dial. This manual method introduces a parallax error. Replacing the dial with an electronic or digital system would eliminate this error.
2. **Leading-Edge Slat Placement:** The leading-edge slat was hand-held, which introduced potential human error in its alignment and stability. Using a mechanical fastener would ensure a more reliable placement of this high lift device.
3. **Pressure Transducer Calibration:** Although the transducer was calibrated at the beginning of the experiment it is still susceptible to systematic errors. However, it is worth noting that a systematic error, in this case, might be preferable to individual errors for each of the 33 pressure taps.
4. **Data Integration with Scanivalve:** The Scanivalve program performs trapezoidal integration to calculate the pressure distribution across the aerofoil from the 33 pressure taps. This method assumes linear change between each of the pressure taps. Increasing the number of pressure taps would reduce this uncertainty and provide a finer resolution of the pressure distribution.
5. **Wind Tunnel Fan Heating:** Extended operation of the wind tunnel fan can lead to overheating, causing inefficiencies in the test section airflow speed. Implementing a cooling system for the fan would mitigate the overheating.

Discussion

According to John D. Anderson [4], aerodynamic lift is derived from the net vertical component of the pressure distribution. From figure 8, we can see how the pressure distribution over an aerofoil changes for attack angles of 2, 8 and 15 degrees. Notably, the net vertical component of pressure grows as the angle of attack increases. This increase in lift is generated by a pressure difference, when the pressure on the bottom layer is high and conversely, the pressure on the upper surface is low.

As John D. Anderson further explains [5], frictional forces acting on a fluid imply that an infinitesimally thin layer of air molecules adjacent to the body sticks to the surface, resulting in zero velocity relative to the surface. As the distance from the surface increases a velocity gradient can be observed where the velocity increases from zero to 99% of the mainstream velocity. This thin region of increasing velocity is known as the boundary layer. At low angles of attack, the boundary layer typically separates at the trailing edge leading to minimal effects on the overall lift generated. However, at greater angles of attack, the boundary layer separates closer to the leading edge of the aerofoil resulting in significant lift loss.

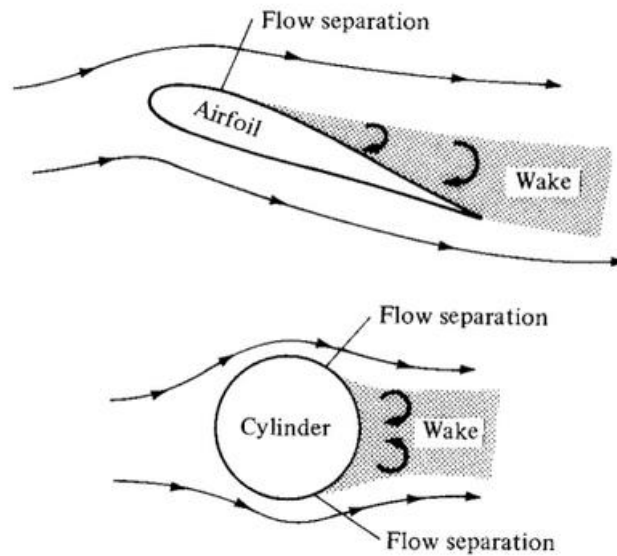


Figure 9 (from John D. Anderson [6]): Visualisation of the principle of flow separation for a viscous fluid over an aerofoil and a cylinder, caused by an adverse pressure gradient region on the surfaces.

This phenomenon is clearly illustrated in figures 6 and 7, where the lift coefficient increases with the angle of attack until it reaches a maximum value, known as the stall point. Beyond this point, the boundary layer separates from the surface leading to a dramatic loss of lift as can be seen from figure 6 when the graph drops sharply. Interestingly, figure 6 highlights that while the linear region of the lift curve remains constant regardless of the Reynolds number, the maximum lift increases with a higher Reynolds number, delaying the stall angle. This is due to the fluid having a larger ratio of inertial to viscous forces, allowing the flow to stick more to the aerofoil surface and delaying flow separation.

When the flow separates from the surface, the pressure distribution is dramatically changed over the surface resulting in a large increase in drag and a loss of lift. Figure 10 introduces how boundary layer separation increases.

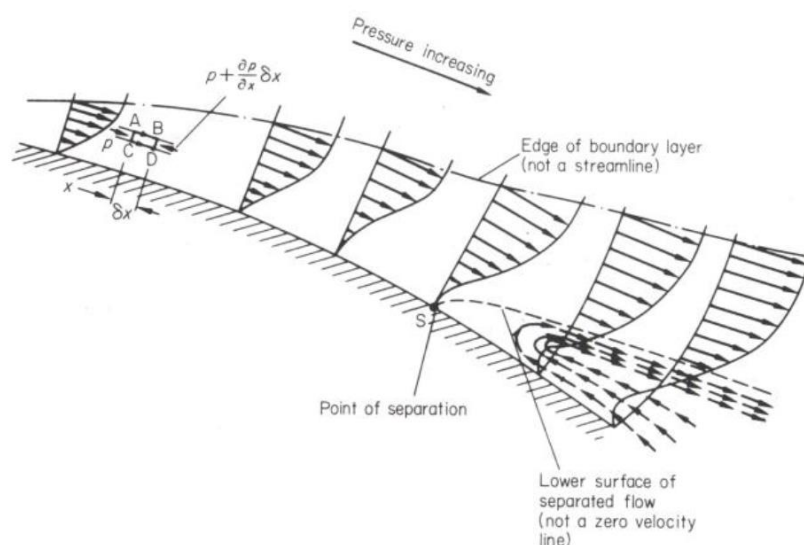


Figure 10 (from the handout [7]): Illustrates how adverse pressure gradients and frictional forces contribute to flow separation in the boundary layer.

In a region of adverse pressure gradient, the fluid elements will slow down as they progress along the surface. These fluid elements, already subject to frictional forces from the boundary layer, come to a

stop somewhere along the surface when their momentum is equal to the forces opposing the fluid elements.

To mitigate flow separation and delay stall, high-lift devices can be employed. During the aerofoil laboratory, a slat was applied on the leading-edge of the aerofoil. As John D. Anderson explains [8], a leading-edge slat allows a secondary flow to take place over the top surface of the aerofoil. This secondary flow injects high momentum fluid into the boundary layer, modifying the pressure distribution over the aerofoil. Figure 8 demonstrates how this pressure distribution over the top surface of the aerofoil is altered. The introduction of a secondary flow mitigates the effect of the adverse pressure gradient which allows for the flow separation over the top surface to be delayed. Therefore, a leading-edge slat increases the stall angle and hence yields a higher maximum lift coefficient, as can be witnessed from figure 7.

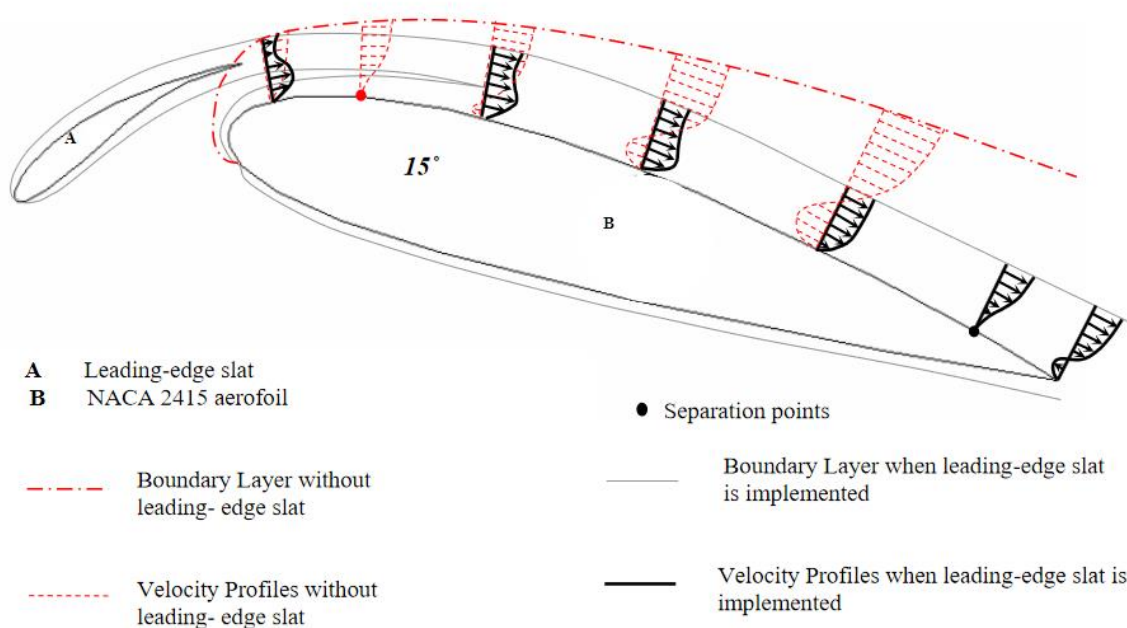


Figure 11 (from the handout [9]): Demonstrates how a leading-edge slat injects high-momentum fluid into the boundary layer, helping to delay flow separation.

Conclusion

In this aerofoil experiment, the pressure distribution over a NACA 2415 aerofoil for a range of angles of attack was measured and pressure bubbles were drawn to visualise the pressure variation. Lift coefficients for a range of angles of attack were recorded and compared with published NACA data. The effect of a leading-edge slat on the lift coefficient was analysed experimentally, demonstrating its ability to enhance lift and delay stall. In conclusion, this study applied fundamental fluid dynamic principles such as boundary layers, pressure coefficients and lift coefficients to gain a deeper understanding of aerofoil performance.

References

- [1] Gary D., 2024. Fluid Dynamics with Historical Notes. Bath. University of Bath
- [2] Arthur B., 2024. Aerofoil Laboratory. Bath. University of Bath
- [3] Department of Mechanical Engineering, 2024. Aerofoil experiment. Bath. University of Bath
- [4] Anderson, J.D., 2017. Fundamentals of Aerodynamics. Sixth edition. New York: McGraw-Hill Education
- [5] Anderson, J.D., 2017. Fundamentals of Aerodynamics. Sixth edition. New York: McGraw-Hill Education
- [6] Anderson, J.D., 2017. Fundamentals of Aerodynamics. Sixth edition. New York: McGraw-Hill Education
- [7] Department of Mechanical Engineering, 2024. Aerofoil experiment. Bath. University of Bath
- [8] Anderson, J.D., 2017. Fundamentals of Aerodynamics. Sixth edition. New York: McGraw-Hill Education
- [9] Department of Mechanical Engineering, 2024. Aerofoil experiment. Bath. University of Bath
- [10] Proofreading. Chat GPT, Open AI, 15th November 2024, <https://chatgpt.com/share/673734b4-9364-800c-b64d-967afb890d49>

Appendix

Laboratory: fluid dynamics of a NACA 2415 aerofoil

Appendix 1: Boeing 747 Questions

Question 1

- a. Calculate the Reynolds number (based on chord) for this experiment. Note the aerofoil chord, $c = 127$ mm and the viscosity of air at 15°C , $\mu = 1.8 \times 10^{-5} \text{ kg m}^{-1} \text{ s}^{-1}$.

$$Re = \frac{\rho V L}{\mu} \Rightarrow \frac{1.225 \times 20 \times 0.127}{1.8 \times 10^{-5}} = 172\,861$$

- b. What was the range of Reynolds numbers for the NACA experiments? Comment.

The Reynolds numbers for the NACA experiments ranged from 3×10^6 to 9×10^6 (a range of 6×10^6). It can be seen that the max. lift co-efficient increases as the Reynolds number increases, as such, the stall point is delayed for a higher Reynolds number. We can also see that the linear region is constant despite the range of Reynolds numbers.

Question 2

A Boeing 747-400 cruises at Mach 0.86 at an altitude of 35,000 feet. At mid-cruise the aircraft weight is 3.20 MN and the total thrust from four engines is 185 kN.

Data at 35,000 feet: static temperature and pressure are 219 K and 23.8 kPa, respectively.

$$(\gamma = 1.4, R = 287 \text{ J/kgK}; \text{ at } 219 \text{ K}, \mu = 1.7 \times 10^{-5} \text{ kg m}^{-1} \text{ s}^{-1})$$

- a. Determine the Reynolds number of the 747, based on a mean chord of 9.0 m.

$$Re = \frac{\rho V L}{\mu} \quad P = \rho R T \Rightarrow \rho = 0.37866 \text{ kg m}^{-3}$$

$$a = \sqrt{\gamma R T} \Rightarrow a = \sqrt{1.4 \times 287 \times 219} = 296.64$$

$$M = \frac{V}{a} \therefore V = 255.1 \text{ ms}^{-1} \quad Re = 51.2 \times 10^6$$

- b. Determine the lift coefficient and lift-to-drag ratio (L/D) if the wing area is 510 m^2 .

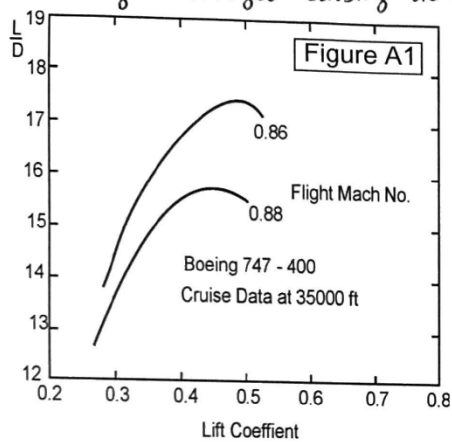
$$\begin{aligned} \text{Lift} &= \text{weight of aircraft} & V &= 255.1 \text{ ms}^{-1} \\ \Rightarrow \text{Lift} &= 3.2 \times 10^6 & \rho &= 0.37866 \text{ kg m}^{-3} \\ \text{Drag} &= \text{thrust for constant velocity} & W &= 3.2 \times 10^6 \\ \Rightarrow \text{Drag} &= 185 \times 10^3 & \Rightarrow C_L &= 0.51 \end{aligned}$$

$$\Rightarrow L/D = 17.3$$

$$C_L = \frac{W}{\frac{1}{2} \rho V^2 S} \quad a = \sqrt{\gamma R T}$$

- c. Compare your calculations with the flight data for the 747-400 shown in Figure A1. With reference to the boundary layer, explain why the lift-to-drag ratio reduces significantly as the Mach number increases from 0.86 to 0.88.

As the Mach number increases from 0.86 to 0.88, approaching transonic speeds, shock waves form on the upper surface of the wing. This shockwave causes the boundary layer to lose momentum and separates from the surface. This separation leads to a large wake that increases drag. When the boundary layer separates due to the shockwave, the pressure distribution on the wing is changed causing the lift to decrease. With the lift decreasing and the drag increasing, the lift to drag ratio reduces significantly.



- d. Due to fuel burn, the weight of the 747 reduces to 2.4 MN when it lands with a sea-level airspeed of 60 m/s using mechanical high-lift devices. ($\rho_{SL} = 1.2 \text{ kg/m}^3$)

Determine the lift coefficient at landing.

$$C_L = \frac{w}{0.5 \rho v^2 s}$$

$$\Rightarrow \frac{2.4 \times 10^6}{0.5 \times 1.2 \times 60^2 \times 510} = 2.18$$

- e. A sketch of typical boundary layer velocity profiles for aerofoils employing mechanical high-lift devices is shown in Figure A2. With reference to the boundary layer, discuss how these slats, vanes and flaps increase lift.

A Leading edge slat increases lift by re-energising the flow on the upper surface of the wing causing a delayed boundary layer separation. This reduces the likelihood of stall, allowing the wing to generate more lift at higher angles of attack.

Flaps increase the wing's effective camber allowing the boundary layer to follow the wing curvature leading to an increase in pressure differential between the upper & lower surfaces. Flaps also allow for the boundary layer to be re-energised, further delaying boundary layer separation.

Figure A2

